Ab Initio Molecular Orbital Study on the Oxidation Mechanism for Dimethylamine Borane as a Reductant for an Electroless Deposition Process

Takayuki Homma,*,† Hiromi Nakai,*,‡ Masaaki Onishi,† and Tetsuya Osaka†

Department of Applied Chemistry and Department of Chemistry, Waseda University, 3-4-1 Okubo, Shinjuku-ku, Tokyo 169-8555, Japan

Received: May 5, 1998; In Final Form: January 8, 1999

The oxidation mechanism of dimethylamine borane (DMAB) as a reductant for an electroless deposition process was studied by an ab initio molecular orbital method. Two types of reaction pathways, via either three-coordinate borane molecules obtained by primary dehydrogenation reactions, or five-coordinate ones by primary additions of OH^- for the oxidation of the DMAB, were examined. While the former pathway corresponds to the general oxidation mechanism of the reductant proposed by Meerakker, the present theoretical results support the latter one. Furthermore, it was clarified that an electron emission occurs when OH^- adds to the four-coordinate compounds, which agrees with the Meerakker's mechanism. Results of the normal-mode analyses showed that the five-coordinate compounds are the transition states. The optimized geometries of monoanion five-coordinate molecules are nearly bipyramidal. The charge and spin-population analyses indicated that the axial bondings in the five-coordinate compounds are stabilized by the three-center three- or four-electron bondings. During the oxidation reaction of the DMAB, the change in the net charge of B is much smaller than that in the formal oxidation number, which is due to a great covalence. The existences of the five-coordinate borane molecules, which are first clarified by the present study, could be the key points of the catalytic activities of the deposited metals.

1. Introduction

Electroless deposition is a technique for formation of metal thin films by reducing metal ions in electrolytes. Unlike the conventional electrodeposition in which external power is necessary to cause the flow of electric current for reducing ions, the electron is supplied from a chemical oxidation reaction of reductant molecules in the electroless deposition. Therefore, this technique can form the metal films not only on conductive substrates but also on nonconductive ones such as plastics and ceramics.

The oxidation process takes place only at the catalytically activated site of the substrate surface. Here, it is notable that the deposited metal itself works as a catalyst. Fine and selective deposition for fabricating microelectronic devices can be achieved by controlling the local catalytic activity. Thus, the most important factors of the electroless deposition are the oxidation of the reductants and the catalytic activities of the deposited metals.[1−3]

A deeper understanding of the deposition reaction should be necessary to achieve precise control of microstructural and functional properties of the deposited films.[4−6] The reaction mechanism has been investigated mainly from electrochemical approaches and kinetic viewpoints.[1−3] An ab initio molecular orbital (MO) method has the capability of providing a mechanistic understanding for the deposition process at an elementary reaction level, which cannot be achieved by the conventional electrochemical approaches. From these points, we focus on the reductants and the catalysts in the electroless deposition process and explore these mechanisms by the ab initio MO method. The present study deals with the former subject, although the latter one will be repeated in the near future.

As for the oxidation reactions of the reductants, Meerakker proposed the following mechanism on the basis of kinetics:[7]

$$RH \xrightarrow{M} \cdot R + \cdot H \qquad \text{Dehydrogenation} \qquad (1)$$

$$\cdot R + OH^- \rightarrow ROH + e^- \qquad \text{Oxidation} \qquad (2)$$

$$\cdot H + \cdot H \rightarrow H_2 \qquad \text{Recombination} \qquad (3)$$

$$\cdot H + OH^- \rightarrow H_2O + e^- \qquad \text{Oxidation} \qquad (4)$$

Here, RH is the reductant. In this mechanism, the first step of the oxidation reactions is a dehydrogenation (eq 1), producing a ·R radical and an atomic hydrogen. It is proposed that this first step determines the catalytic nature of the electroless deposition processes. As shown in eq 2, an electron is produced from the oxidation of the ·R radical. Depending on the metal species, which catalyze the reaction, the hydrogen atom gives either H_2 gas (eq 3) or H_2O (eq 4).

Dimethylamine borane (DMAB; $(CH_3)_2NHBH_3$), which is the typical reductant, leads to the stepwise oxidation reactions, yielding four-coordinate borane molecules of $BH_{4-n}(OH)_n^-$ ($n = 1-4$). According to Meerakker's mechanism, DMAB is expected to produce three-coordinate borane radicals such as $\cdot BH_2(OH)^-$, $\cdot BH(OH)_2^-$, and $\cdot B(OH)_3^-$ by dehydrogenation reactions.[7] However, the existence of any intermediates except the four-coordinate BH_3OH^- compound was not suggested by previous experimental studies.[7−12] From the experimental dif-

* Authors to whom correspondence should be addressed. E-mail: homma@mse.waseda.ac.jp.
† Department of Applied Chemistry.
‡ Department of Chemistry.

10.1021/jp982116b CCC: $18.00
Published on Web 02/20/1999

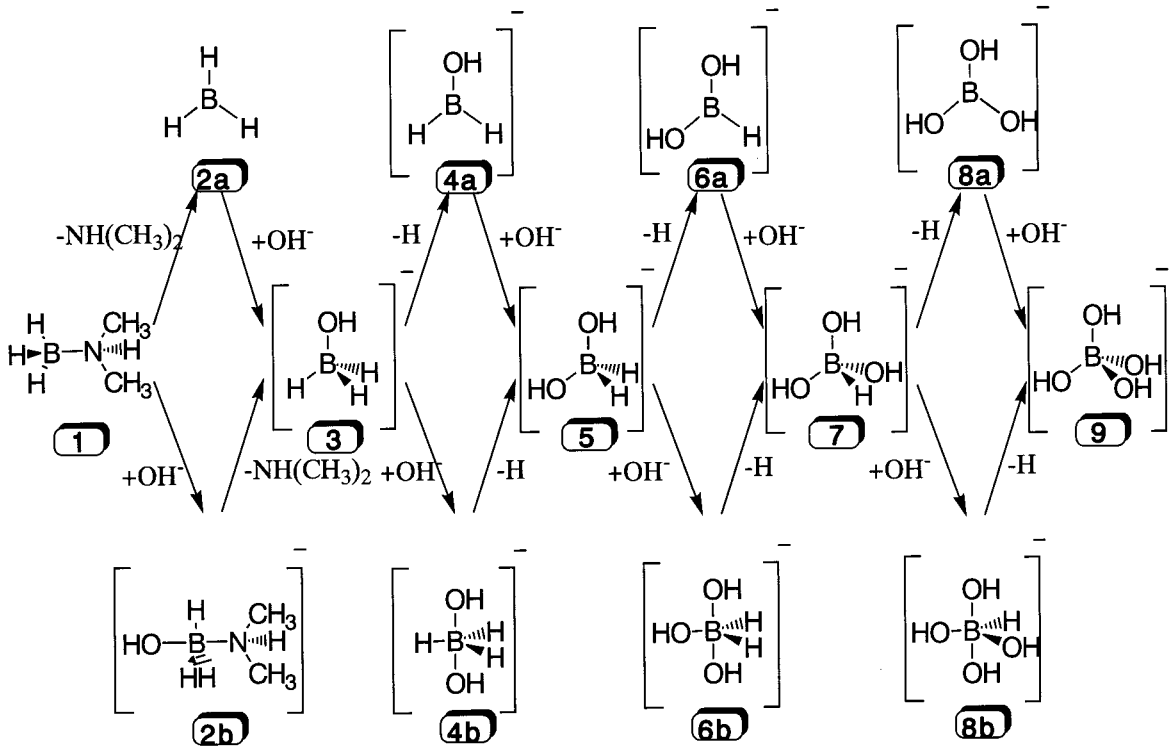

Figure 1. The reaction pathways via three-coordinate and via five-coordinate.

ficulty in determining intermediates, we have theoretically investigated the stabilities of the above intermediates and further clarified the oxidation mechanism of the DMAB reductant.

2. Computational Method

An electroless deposition reaction takes place at the solid/liquid interface, thus the reaction is influenced by a numbers of factors, such as catalytic activities of the deposited metals and a solvation effect. Since this work is the first trial for the theoretical investigation of the electroless deposition reaction, we try to start from a simple system, i.e., to clarify the oxidation mechanism of DMAB in the gas phase by the ab initio MO method. The solvation effect is considered to be small because of the cancellation of the effect on both sides of eq 2. We discuss the details in the third paragraph.

We assume two pathways from DMAB to $B(OH)_4^-$ as shown in Figure 1. Namely, one is via three-coordinate borane molecules obtained by primary dehydrogenation reactions, and the other is via five-coordinate ones by primary additions of OH^-. The former corresponds to Meerakker's mechanism in the gas phase.[7]

The geometries of these molecules are all optimized at the Hartree−Fock (HF) level. The electron correlations are taken into account for the single-point energy calculations by the second-order Møller−Plesset perturbation (MP2) method. We further carry out the normal-mode analyses for the optimized molecules to determine whether they are intermediates or transition states (TSs). The calculations are performed using the GAUSSIAN94 software package.[13] The Gaussian basis sets used in the present calculations are so-called D95V ones; that is, (9s5p)/[3s2p] sets for B, C, N, and O and (4s)/[2s] set for H.[14−17]

3. Results and Discussion

Figure 2 shows the energy diagram for the oxidation reactions of DMAB; the reaction proceeds from left to right, and the energy is shown in kcal/mol relative to that of DMAB. The energy level of a produced electron is defined at zero. Two energy levels correspond to the two reaction pathways via either three- or five-coordinate borane molecules, as shown in Figure 1. The change in energy level indicates that the stepwise oxidation reactions of DMAB proceed exothermically via four-coordinate borane molecules $BH_{4-n}(OH)_n^-$ ($n = 1-4$). However, the processes from these four-coordinate compounds to the three- or five-coordinate ones are endothermic. On the whole, exothermic reactions proceed naturally.

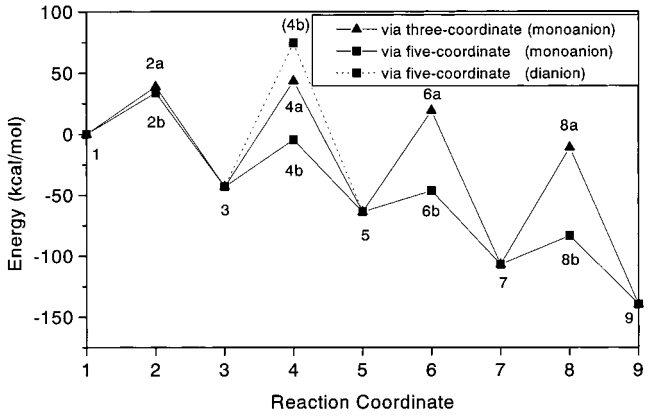

Figure 2. The energy diagram for the reaction of DMAB handled by the ab initio Hartree−Fock molecular orbital method.

The first step from DMAB (**1**) to $BH_3(OH)^-$ (**3**), which does not accompany the oxidation of boron, is a ligand replacement reaction from dimethylamine to OH^-. The energy difference between three- and five-coordinate compounds, namely, **2a** and **2b**, is calculated to be only 5.0 kcal/mol. On the other hand, in the second step from $BH_3(OH)^-$ (**3**) to $BH_2(OH)_2^-$ (**5**), the energy level of the five-coordinate compound (**4b**) is about 48.0 kcal/mol lower than the three-coordinate one (**4a**). Such energy profiles are quite similar to those in the third and fourth steps, namely, **5** → **7** and **7** → **9**, respectively.

The question we have to ask here is the solvation effect and the value of the energy given to the electron. For example, in the step from **3** → **5**,

$$BH_3(OH)^- + OH^- \rightarrow BH_2(OH)_2^- + \cdot H + e^- \qquad (5)$$

we compare the solvation stabilization of OH^- and the stabilization of the electron. Considering that the solvent is water, the solvation stabilization of the former is about 5.0 eV.[18] On the other hand, the stability of an electron at 0 V on the electrochemical scale, measured with respect to the standard hydrogen electrode, is about 4.6 eV on the physical (vacuum) scale.[19] Palladium is a possible candidate for the electroless deposition and the standard potential for Pd^{2+} reduction in water is 0.92 V on the electrochemical scale, which corresponds to 5.52 eV on the vacuum scale. Thus, both sides of eq 5 are stabilized at about 5 eV when the bonding of OH^- and e^- to their environment are taken into account. The difference in solvation energy for $BH_3(OH)^-$ and $BH_2(OH)_2^-$ should be small. Other possible depositioning cations have different reduction potentials, for example −0.23 V for Ni^{2+}, which would decrease the sequential stabilities, but still allow reactivity. Thus, we neglected the solvation effect in this paper.

Figure 2 also shows the energy levels of the $BH_3(OH)_22^-$ dianion in the broken line, which is directly led by an addition of OH^- to $BH_3(OH)^-$ (**3**). However, this energy level is much higher than that of the $BH_3(OH)_2^-$ monoanion, indicating that one electron is emitted from the reductant when OH^- is added to the four-coordinate borane compounds.

By the normal-mode analysis, all five-coordinate compounds are found to be transition states (TSs), whereas all three-coordinate ones are energy minima. The mode for the negative eigenvalue corresponds not only to the addition of OH^- but also to the elimination of H. The ligand replacement reactions of the four-coordinate borane compounds from H to OH occur as one step, at which the TSs are the five-coordinate ones. Therefore, these processes seem to be S_N2 reactions. The S_N2 reaction means "Substitution Nucleophilic Bimolecular reaction". It should be noted that the direction of the elimination is not normal in comparison with the usual S_N2 reaction. Namely, the H atom eliminates from the equatorial position.

The present reaction mechanism via the five-coordinate compounds as the TSs does not agree with the Meerakker's mechanism. Although he proposed that the dehydrogenation occurs as the first step, the present results indicate that the addition of OH^- occurs before or at the same time as the dehydrogenation. However, two mechanisms agree in the point that the electron is emitted in the OH^- addition step.

Next, we compare the chemical bondings of the three-, four-, and five-coordinate borane molecules. In all four-coordinate compounds, $BH_{4-n}(OH)_n^-$ ($n = 1-4$), the bond angle between boron and ligands are about T_d angle, which is due to the sp^3 hybridization. The three-coordinate compounds are nearly planer and have the L−B−L′ (L, L′ = H or OH) angles of 107.1°−117.1°. The electronic structures of boron in these compounds correspond to the sp^2 hybridization. Note that the charge and spin occupations of the out-of-plane p_z AO of B are 0.722−0.979 and 0.404−0.723, respectively.

Figure 3 shows the optimized geometries of the five-coordinate compounds. These compounds are nearly bipyramidal. However, the O_{a1}−B−O_{a2} angles are bent from the linear; namely, 169.3°, 156.9°, and 151.7° for **4b**, **6b**, and **8b**, respectively.

It is notable that a B−H bond length of 1.35 Å for **8b** is longer than the usual length of 1.20 Å. This extra B−H bond

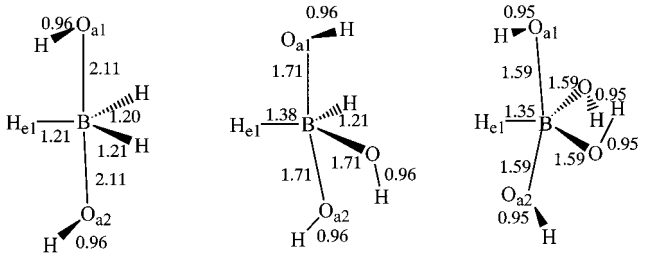

Figure 3. The optimized geometries of the five-coordinate compounds.

TABLE 1: Mulliken Charge Populations of B, O_{a1}, and O_{a2}

		$BH_3(OH)_2^-$	$BH_2(OH)_3^-$	$BH(OH)_4^-$
B	s	3.051	2.841	2.652
	p_x	1.004	0.520	0.600
	p_y	0.878	0.816	0.584
	p_z	0.416	0.460	0.609
O_{a1}	s	3.914	3.880	3.845
	p_x	1.364	1.610	1.454
	p_y	1.995	1.663	1.895
	p_z	1.352	1.460	1.505
O_{a2}	s	3.914	3.864	3.832
	p_x	1.364	1.843	1.702
	p_y	1.995	1.594	1.738
	p_z	1.352	1.571	1.503

TABLE 2: Mulliken Spin Populations of B, O_{a1}, O_{a2}, and H_{e1}

		$BH_3(OH)_2^-$	$BH_2(OH)_3^-$	$BH(OH)_4^-$
B	s	−0.082	0.001	−0.032
	p_x	−0.032	0.012	−0.008
	p_y	−0.045	0.011	0.000
	p_z	−0.315	−0.057	−0.052
O_{a1}	s	0.021	0.015	0.008
	p_x	0.037	0.046	0.029
	p_y	0.001	0.152	0.029
	p_z	0.607	0.316	0.168
O_{a2}	s	0.021	0.005	0.012
	p_x	0.037	0.008	0.029
	p_y	0.001	0.002	0.012
	p_z	0.607	0.055	0.125
H_{e1}	s	0.092	0.483	0.698

corresponds to the stretching mode in the TS, as mentioned above. The bond of B with the three equatorial ligands are due to sp^2 hybridization in the five-coordinate compounds as well as in the three-coordinate ones. The axial bonds are due to the coordinate bonds of the two OH groups.

Table 1 shows the Mulliken populations of B, O_{a1}, and O_{a2} in **4b**, **6b**, and **8b**, respectively. Here, the B−O_{a1} bond is set to the *Z*-axis. The p_z populations of B are 0.416−0.609, which are smaller than those in the three-coordinate compounds. The sums of the p_z populations of B, O_{a1}, and O_{a2} slightly increase by replacing the equatorial ligand from H to OH, although they are about three; namely, 3.12, 3.49 and 3.62 for **4b**, **6b**, and **8b**, respectively.

Table 2 shows the spin populations of B, O_{a1}, O_{a2}, and H_{e1}. The H_{e1} atom corresponds to the H atom in the equatorial position. Most parts of the spin, which is one in **4b**, **6b**, and **8b**, exist in the p_z AOs of these four atoms. The spin population of p_z AO of B is smaller than those of O_{a1} and O_{a2}. As there is an increase in the p_z charge populations of B, O_{a1}, and O_{a2}, the spin populations of these atoms decrease, transferring the spin to the equatorial H_{e1} atom.

On the basis of the charge and spin population analyses, the axial bonds are found to be three-center three- or four-electron bonds, which are illustrated in Figure 4. As well-known, the

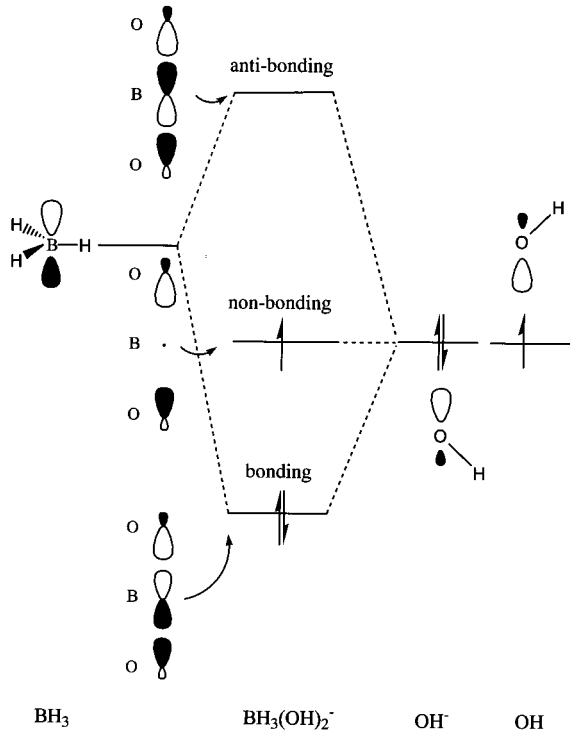

Figure 4. Schematic orbital correlation diagram between BH_3 and two OH groups. Three-center three-electron bonding interaction is seen in the axial O−B−O bond of the five-coordinate $BH_3(OH)_2^-$ molecule.

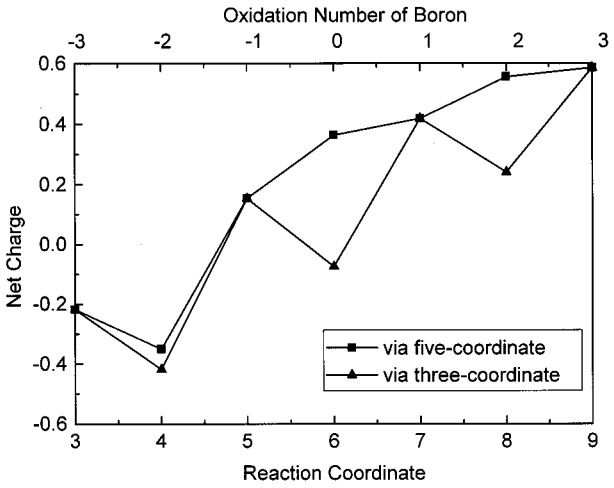

Figure 5. The change in the net charge of B along the reaction coordinate.

lowest MO in the three-center bond has a bonding nature. The stabilization due to this bonding MO seems to lead to the stabilization of the five-coordinate compounds compared with the three-coordinate ones. The increase in the p_z charge populations only changes the occupation of the nonbonding MO, which may not bring about the large stabilization or lack of stabilization.

The above theoretical results have clarified that despite the great change in the oxidation number of boron, i.e., −3 to +3, a series of the structure and energy changes occur repeatedly in the stepwise oxidation reactions of DMAB. Figure 5 shows the net charge of B along the reaction coordinate. The oxidation number of B is also shown on the horizontal axis of the upper side. Two changes correspond to the two reaction pathways via three- and five-coordinate compounds, respectively.

The absolute values of the net charges are much smaller than those of the oxidation numbers; that is, −0.4 to +0.6 for the former and −3 to +3 for the latter, which is due to the great covalence in the chemical bonds of these borane molecules. Therefore, even the boron atoms with different oxidation numbers can make the sp^3 or sp^2 hybridization, and bring about similar structures.

The changes in the net charges from the four-coordinate compounds to the three-coordinate ones are opposite to those in the oxidation numbers; namely, −0.22 → −0.42, +0.15 → −0.07, and +0.42 → +0.24 for **3** → **4a**, **5** → **6a**, and **7** → **8a**, respectively. On the other hand, these changes agree with each other along the reaction pathway via the five-coordinate compounds, although that of **3** → **4b** shows an opposite change of −0.22 → −0.35. Such a natural change in the net charge of B strongly indicates the reasonable reaction pathway via the five-coordinate compounds.

Conclusion

We have studied the oxidation mechanism of the DMAB reductant for the electroless deposition by the ab initio MO method. Two types of reaction pathways, either via three-coordinate or five-coordinate borane molecules, were examined. The obtained results support the latter pathway. The electron emission from the reductant is expected to occur at the same time as the addition of OH. It is also suggested that the stabilization of the five-coordinate compounds rather than the three-coordinate ones are due to the axial bonds by OH groups. The charge and spin population analyses indicate that the axial bonds are the three-center three- or four-electron bonds. Great covalence exists in the chemical bonding of the borane molecules.

As described, it is demonstrated that the ab initio MO method is a powerful tool for investigating the mechanism of the electroless deposition in detail. Since the present theoretical study is the first trial, the effect of metal surface, which is expected to work as a catalyst, is not taken into consideration. Without the metal surface, the energy barriers are not so small even for the reaction pathway via the five-coordinate borane molecules, of which the existences are first proposed by the present theoretical study. Therefore, it is suggested that the stabilities of the five-coordinate borane molecules could play the key role for the catalytic activities.

Acknowledgment. The present calculations were performed using the computers at the Media Network Center (MNC) of Waseda University. This study was supported in part by the Grant-in-Aid for Scientific Research from the Ministry of Education, Science, and Culture of Japan, The Kurata Foundation, and by the Waseda University Grant for Special Research Projects. The authors thank Dr. Masanori Tachikawa for his valuable comments. The authors acknowledge one of the reviewers for the valuable suggestion about the solvation effect.

Appendix: Accuracy of the Present Calculation Method

We show here the accuracy of the present basis functions and the effects of electron correlations. In the oxidation reaction of DMAB, the oxidation number of boron changes from −3 to +3. Furthermore, the intermediates of **3** to **9** are anions. Thus, we should check the accuracy of the basis function of B at first; especially, the effect of adding the anion basis functions to B.

Table 3 compares the following reaction heat from **3** to **5** calculated at the HF level,

$$BH_3(OH)^-\ (\mathbf{3}) + OH^- = BH_2(OH)_2^-\ (\mathbf{5}) + H + e^- - Q$$

TABLE 3: Effect of Adding Diffuse Functions to B at the HF Levels

basis sets	Q_{ex}[a] (kcal/mol)	Q_{in}[a] (kcal/mol)	$Q_{in} - Q_{ex}$ (kcal/mol)
D95V[b]	−29.7	−31.9	−2.2
cc-pVDZ[c]	−37.8	−39.1	−1.3
cc-pVTZ[c]	−41.5	−43.2	−1.7
cc-pVQZ[c]	−42.8	−45.4	−2.6
$Q = E(BH_2(OH)_2) + E(H) - E(OH^-) - E(BH_3OH^-)$			

[a] Q_{ex} and Q_{in} mean excluding and including diffuse functions, respectively. [b] Huzinaga−Dunning valence double-ζ basis set.[14] [c] Dunning's correlation consistent basis sets (double, triple, and quartet-ζ respectively). These basis sets include polarization functions.[15−17]

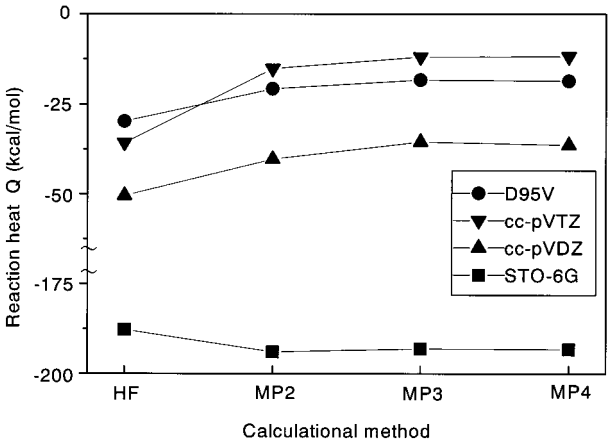

Figure 6. Correlation effect for the reaction heat from **3** to **5**.

where the energy level of the free electron is set to zero. The energy shifts by adding the diffuse functions are found to be quite small; that is, less than 3 kcal/mol. While the reaction heat gradually increases by using higher-level basis sets, it is shown that the energy changes are not too large.

Next, the correlation effects are examined by using the HF and the second-, third-, and fourth-order MP (MP2, MP3, MP4) methods. The basis sets for all atoms are changed from minimal to triple-ζ+ polarization classes. Figure 6 shows the above-mentioned reaction heat from **3** to **5** with the different bases and at the different calculation levels. Rapid convergences of correlation effects are seen for all bases. For example, the difference between the MP2 and MP4 results with the D95V basis, 2.2 kcal/mol, is smaller than that between the HF and MP2 ones, 9.0 kcal/mol. Figure 6 further means that the usage of the STO-6G basis is not suitable, even by the correlation methods.

Considering the results shown in Table 3 and Figure 6, the MP2 calculations with the D95V basis even excluding a diffuse function give reasonable energetic results. Therefore, we have adopted this method in the calculations of the text. Of course, the MP4 calculations with larger basis sets such as cc-pVQZ may give better results than the present choice. However, the improvements are rather small, verifying the present choice for minimizing computer time.

Finally, we show the numerical data for the total energies of all molecules in Table 4. These data are calculated by the MP2 method with the D95V basis, which corresponds to the present choice in the text. The relative energies with respect to compound **1** are also shown in Table 5. There, the energy level of the free electron is set to zero in the usual way. These data

TABLE 4: Calculated Total Energies of the Molecules (hartrees)

molecules	E_{HF}	E_{MP2}
OH^-	−75.347203	−75.477416
H	−0.497637	−0.497637
$(CH_3)_2NHBH_3$	−160.619392	−160.965045
$(CH_3)_2NH$	−134.200365	−134.47680
BH_3	−26.376170	−26.426231
$(CH_3)_2NHBH_3OH^-$	−235.914293	−236.37247
BH_3OH^-	−101.846741	−102.034253
BH_2OH^-	−101.223485	−101.39882
$BH_3(OH)_2^-$	−177.151269	−177.450474
$BH_2(OH)_2^-$	−176.747601	−177.048236
$BH(OH)_2^-$	−176.126824	−176.417343
$BH_2(OH)_3^-$	−252.059153	−252.496784
$BH(OH)_3^-$	−251.678297	−252.095585
$B(OH)_3^-$	−251.041356	−251.445214
$BH(OH)_4^-$	−326.981209	−327.535743
$B(OH)_4^-$	−326.601123	−327.130542

TABLE 5: Calculated Relative Energies of the Molecules (kcal/mol)

molecules	E_{HF}	E_{MP2}
1	0	0
2a	26.89	38.91
2b	22.82	33.92
3	−50.52	−43.04
4a	28.31	43.42
4b	−23.74	−4.64
5	−80.26	−63.81
6a	−5.44	19.11
6b	−60.34	−46.39
7	−133.62	−106.91
8a	−46.20	−11.07
8b	−105.83	−83.53
9	−172.19	−139.55

may be helpful for other researchers in order to repeat similar calculations and/or to compare results using different methodologies.

References and Notes

(1) Mallory, G. O.; Hajdu, J. B. *Electroless Plating. Fundamentals and Applications*; American Electroplaters and surface Finishers Society: Orland, **1990**.

(2) Ohno, I. *Mater. Sci. Eng.* **1991**, *A146*, 33.

(3) Haruyama, S.; Ohno, I. *Electrochem. Soc. Proc.* **1988**, *PV88−12*, 20.

(4) Brusic, V.; Horkans, J.; Barclay, D. J. *Advances in Electrochemical Science and Engineering*; VCH: Weinheim, 1990; Vol. 1, p 249.

(5) Osaka, T.; Homma, T. *New Trends and Approaches in Electrochemical Technology*; Kodansha and VCH: Tokyo and Weinheim, 1993; p 13.

(6) Okinaka, Y.; Osaka T. *Advances in Electrochemical Science and Engineering*; 1994; *3*, 55, VCH: Weinheim, 1994; Vol. 3, p 55.

(7) Van den Meerakker, J. E. A. M. *J. Appl. Electrochem.* **1981**, *11*, 397.

(8) Elder, J. P.; Hickling, A. *Trans. Faraday Soc.* **1962**, *58*, 1852.

(9) Elder, J. P. *Electrochim. Acta* **1962**, *7*, 417.

(10) Holbrook, K. A.; Twist, P. J. *J. Chem. Soc. (A)* **1971**, *7*, 890.

(11) Gardiner, J. A.; Collat, J. W. *Inorg. Chem.* **1965**, *4*, 1208.

(12) Gardiner, J. A.; Collat, J. W. *J. Am. Chem. Soc.* **1965**, *4*, 1693.

(13) Frisch, M. J.; Gordon, M. H.; Trucks, G. W.; Foresman, J. B.; Schlegel, H. B.; Raghavachari, K.; Robb, M. A.; Binkly, J. S.; Gonzalez, C.; Defrees, D. J.; Fox, D. J.; Whiteside, R. A.; Seeger, R.; Melius, C. F.; Baker, J.; Martin, R. L.; Stewart, J. J. P.; Topol, S.; Pople, J. *GAUSSIAN94*; Gaussian Inc.: Pittsburgh, PA, 1994.

(14) Huzinaga, S. *J. Chem. Phys.* **1965**, *42*, 1293. Dunning, T. H., Jr. *J. Chem. Phys.* **1970**, *53*, 2823.

(15) Woon, D. E.; Dunning, T. H., Jr. *J. Chem. Phys.* **1993**, *98*, 1358.

(16) Kendall, R. A.; Dunning, T. H., Jr.; Harrison, R. J. *J. Chem. Phys.* **1992**, *96*, 6796

(17) Dunning, T. H., Jr. *J. Chem. Phys.* **1989**, *90*, 1007.

(18) The Chemical Society of Japan *Kagaku-binran* **1984**, *2*, 336

(19) Bockris, Khan, *Surface Electrochemistry, A Molecular Level Approach*, **1993**, 78.